Structures and Ore Genesis of the Grimsdalen Sulphide Deposits, Southern Trondheim Region, Norway

STIG ASBJØRN SCHACK PEDERSEN

Pedersen, S. A. S. 1979: Structures and ore genesis of the Grimsdalen sulphide deposits, southern Trondheim region, Norway. *Norges geol. Unders. 351*, 77–98.

The central part of the Grimsdalen area of the southern Trondheim region is occupied by a sequence of metavolcanics with subordinate metasediments, termed the Folla Group, which are correlated with the Støren Group of the central and western parts of the region. The Folla Group is thrust above arkosic sparagmites and is itself overthrust by metasediments of the Mesæterhø Group. A tectonic model for the Grimsdalen area, which has been affected by two major phases of deformation, is presented. The sulphide deposits of the area occur in a single pyritite horizon within the Folla Group, and 4 ore types have been differentiated. The metamorphic evolution of the pyritite and the different generations of pyrite are discussed in relation to the structural and metamorphic history of the Folla Group sequence.

S. A. Schack Pedersen, Institut for almen Geologi, Østervoldgade 10, 1350 København K

Introduction

The Grimsdalen area lies 10 km south-west of the Folldal ore field in the southern part of the Trondheim region. The thrust boundary between the deformed mica schists and greenschists of the Trondheim Nappe (Wolff 1967) and the sparagmites of the underlying Kvitvola Nappe (Heim 1971, Strand 1972) passes through the southern part of the area (Plate 1). The sulphide ore deposits in Grimdalen form a continuation of the known ore field around Folldal (Foslie 1926), which belongs to the large group of stratiform sulphide deposits of the Scandinavian Caledonides (Oftedahl 1958, Vokes 1968, 1976).

The area has been affected by two main deformations, both characterized by greenschist to amphibolite facies conditions. In this paper a model for the structural development is presented. It is shown that the concentration of the stratiform sulphides into ore bodies occurred during the first major deformation while the actual present-day location of the ore bodies is governed by the second phase of deformation. The structural model makes it possible to predict the subsurface position of the ore bodies.

Lithology and field relations of the major units

The rocks of the Grimsdalen area can be divided informally into three larger tectono–stratigraphic units: the sparagmites, the Folla Group and the Mesæterhø Group (Fig. 1).

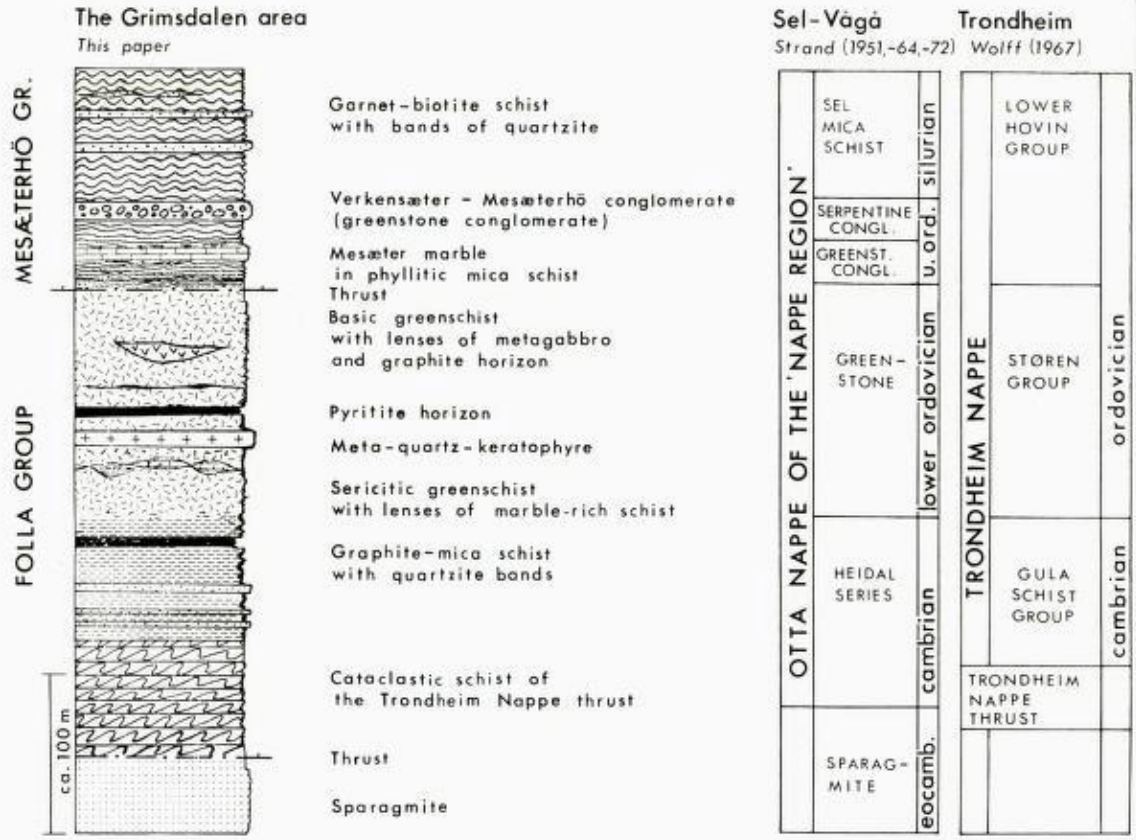

Fig. 1. Tectonostratigraphic column for the Grimsdalen area.

THE SPARAGMITES

The sparagmites of the Grimsdalen area lie along the northern border of the Rondane mountains. The rocks are grey to pale grey quartzites or meta-arkoses frequently containing epidote and specular hematite. Quartz is often segregated into quartz rods parallel to the main fold axes. The general dip is 20°–30° to the north-west and fold axes plunge 20° to the west.

THE THRUST ZONE BETWEEN THE SPARAGMITES AND THE FOLLA GROUP

The border between the sparagmites and the overlying Folla Group is part of the major thrust beneath the Trondheim Nappe (Wolff 1967). The thrust is marked by a sequence of mylonitic rocks which in accordance with Higgins (1971) may be termed mylonitic schists, mylo–sparagmite, magnetite–porphyroblast mylonite with banded intercalations of a black phyllonitic schist with ilmenite porphyroblasts, breccia mylonite and metagabbro mylonite. From this it is evident that the mylonite zone is a lithologically variegated zone.

The general dip of the thrust plane is to the NNW east of Sjøberget, and to the NW west of Sjøberget. Overturned antiforms of the Folla Group rocks

have been upthrusted against the mylonite zone along thrust planes dipping ca. 50°NW.

THE FOLLA GROUP

The metavolcanics extending from Kakelldalen in the east to the watershed between Grimsdalen and Gudbrandsdalen to the west were named by Heim (1971) the Folla Group after the river Folla in Folldal. The group has been correlated with the Lower Ordovician Støren Group (Vogt 1945) of the central part of the Trondheim region (Heim 1971).

The Folla Group makes up the central part of the Grimsdalen area and has a thrust boundary with the overlying Mesæterhø Group and with the underlying sparagmites (Plate 1). In the Grimsdalen area the Folla Group can be divided into the following units (Fig. 1).

Basic greenschist (structurally highest)
(containing the pyritite horizon)
Meta–quartz–keratophyre
Sericitic greenschist
Graphite–mica schist (structurally lowest)

For reasons that are given later, the sequence is believed to be inverted.

Basic greenschist

This unit consists of alternating layers of amphibolite, fine-grained hornblende greenschist and hornblende–chlorite greenschist. A plane-parallel orientation of hornblende forms the schistosity in all the rocks. Plagioclase is generally an albite, but andesine has been found in a few samples of amphibolite and as porphyric grains in a metabasite from the hinge zone of a fold formed during the early fold phase (F_{D2}, see later). On fold flanks this metabasite has been transformed into an albite–chlorite greenschist with chlorite pseudomorphs after hornblende and zoisitization of the plagioclase grains. Within the lowest 10 m of the basic greenschist occurs a rock consisting of more than 50% pyrite, hereafter called pyritite (Schermerhorn 1970). The present thickness of the pyritite varies from 10 cm to 2 m, and in isoclinal early fold closures it forms ore bodies with an average thickness of 4 m.

The pyritite is seldom exposed in the field, but it is known from the abandoned Grimsdal mine and from a series of diamond drill cores drilled by Folldal Verk A/S in the years 1970–1976 (Fig. 2).

Metagabbro is found in the middle of the basic greenschist. The gabbro was intruded as sills or dykes and has locally been transformed into lensoid actinolite aggregates up to 5 metres in size. At Sjøberget a larger body of metagabbro occurs. To the southwest this body is strongly mylonitized where it abuts against the Trondheim Nappe thrust.

Graphitic schists occur as up to 30 cm-wide bands in the fine-grained horn-

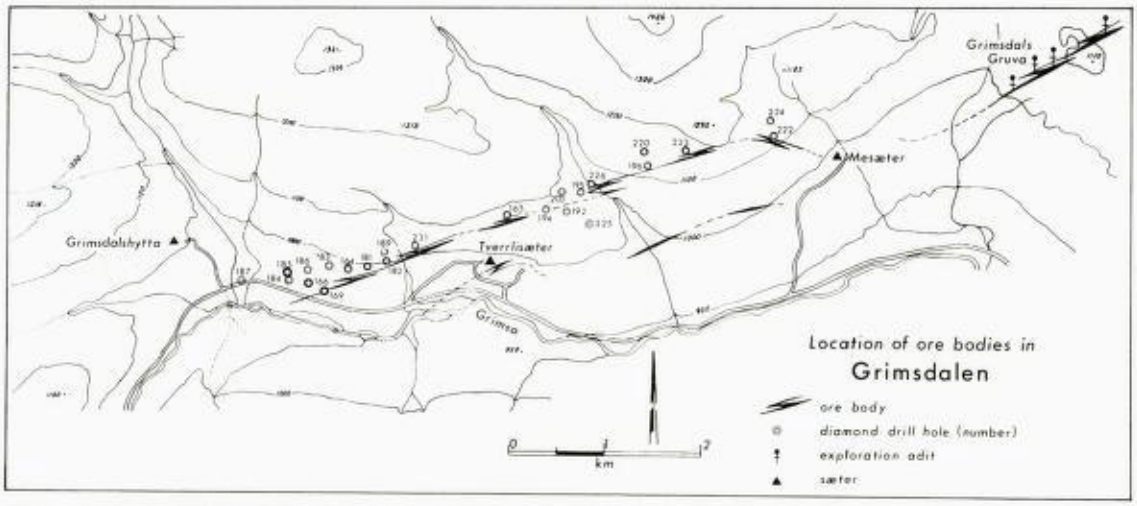

Fig. 2. Location of the ore bodies in Grimsdalen. Based on data from diamond drill cores (Folldal Verk A/S), geophysical investigation and geological mapping.

blende–chlorite greenschist. This alternation between metasediments and metavolcanics makes it probable that the whole sequence of amphibolites and greenschists represents a series of submarine metavolcanics.

Meta–quartz–keratophyre

This rock crops out as a light, resistant rock often forming terraces or ridges in the landscape. The rock is whitish, but can have a yellowish tint due to corrosion of small (0.5 mm) pyrite idioblasts.

Hornblende porphyroblasts form star-like aggregates, and at the contact to the basic greenschist these may develop into garbenschiefer. Garnet porphyroblasts are abundant, and along the contact to the sericitic greenschist the meta–quartz–keratophyre is developed as a snowball-garnet schist, where the rotated garnets can reach a size of 5 cm in diameter. The main minerals are quartz and albite forming a fine-grained granoblastic matrix which is a result of mylonitization. A few larger grains of oligoclase have been found; these contain a lot of inclusions and have corroded boundaries indicating a pyroclastic origin for the rock.

The submarine–sedimentary origin of the lithology is documented by the existence of 1–10 cm-wide graphite bands interbedded with meta–quartz–keratophyre at the transition to the sericitic greenschist.

Tectonically the meta–quartz–keratophyre behaves like a competent layer between the basic and the sericitic greenschists. It often forms characteristic buckle-type folds in hinge zones, while it is boudined on fold flanks. Boudinage combined with compression, shearing-out and metamorphic transformation can locally have transformed the meta–quartz–keratophyre to a foliated quartz–hornblende–plagioclase schist.

Sericitic greenschist

This unit consists of light green or grey-green, fine-grained greenschists characterized by their content of sericite and by the bright green mineral fuchsite. The greenschists are strongly tectonised and kink folds are common. Yellowish to pale brown carbonaceous mica schists are interbedded in the unit, and close to the contact to the meta–quartz–keratophyre a carbonate-banded grey mica schist appears locally. These rocks are interpreted as metasediments, representing sedimentary intercalations in a series of metavolcanics.

Graphite–mica schist

A graphite–mica schist which grades into a quartzite-banded mica schist has a concordant contact to the sericitic greenschist. The quartzite-banded mica schist is seldom exposed, but the graphite schist is often found intensively infolded in the sericitic greenschist.

Wolff (1967) and Heim (1971) correlate the Mesæterhø Group (this paper) with the Gula Group. As the graphite–mica schist in Grimsdalen tectonically belongs to the Folla Group, which is separated by a thrust zone from the Mesæterhø Group, it is proposed that the unit belongs to the Folla Group.

THE THRUST ZONE BETWEEN THE FOLLA AND MESÆTERHØ GROUPS

The mylonitic rocks of this zone can be related to either the overlying Mesæterhø Group or the underlying Folla Group. In the Folla Group the basic greenschists have been altered to cataclastic greenschist with hornblende cataclasts surrounded by chlorite forming a mylonite schistosity. Near the thrust the meta–quartz–keratophyre has been transformed into leucocratic breccia mylonite. A phyllonitic greenschist with a green silky sheen is regarded as being the mylonitic equivalent of the sericitic greenschist, but as the meta–quartz–keratophyre is boudined and sheared-out, it is impossible to differentiate the tectonically mixed greenschists.

The rocks of the upper contact are mostly fine-grained, grey mica schists (phyllonitic) or red-grey, strongly sheared, biotite–chlorite schists. North of Mesæter a silver-grey to dark grey mylonite schist appears with intercalations of Mesæter marble (see later).

The general orientation of the thrust is shown in stereogram 2 in Plate 1. The fold axes have been sheared out during the thrusting and lie on a great circle, which corresponds to the plane representing the orientation of the thrust.

THE MESÆTERHØ GROUP

The Mesæterhø Group makes up the northern part of the mapped area and has previously been described by Heim (1971) under the name Gula Group. As the lithostratigraphic correlations between the southern Trondheim region and the type area of the Gula Group have been much discussed (Bugge 1954, Strand 1951, 1960, 1972, Wolff 1967) the present author prefers to use a more local designation. The name Mesæterhø Group is strictly informal.

The main rock-type of the Mesæterhø Group is a grey-brown to rust-col-

oured garnet–biotite schist. Garnets frequently form up to 0.5 cm-sized porphyroblasts that have been rotated, flattened, and often altered to chlorite. Staurolite idioblasts are locally abundant, and kyanite has been found as sheaf-like aggregates up to 5 cm long. Due to retrograde metamorphism staurolite and kyanite may be altered to sericite pseudomorphs.

In the structurally highest part of the mica schists metre-thick intercalations of arkosic quartzite occur. In the structurally lowermost part of the group two important units appear: a meta-conglomerate and a marble horizon, both previously described by Bjørlykke (1905) from Verkensæter in Grimsdalen.

The meta-conglomerate varies in lithology laterally, but as the matrix generally consists of amphibole ± chlorite it may be termed a greenstone conglomerate (Strand 1951). The clasts are dominated by quartzo–feldspathic rocks which may contain hornblende needles in which case they resemble meta–quartz–keratophyre. Amphibolite–greenstone clasts are common and holes with a rim of hematite/goethite indicate that clasts with a high content of sulphides have been present. Thus, most of the rocks of the Folla Group are represented in the conglomerate.

As a result of deformation the pebbles are flattened and elongated, and in strongly deformed meta-conglomerates the quartzo–feldspathic pebbles form a leucocratic banding in a cataclastic hornblende schist.

The marble unit ('der Mesæter Marmor' of Heim, 1971) forms a 1–12 m-thick layer in a series of grey phyllitic mica schists in the lowest part of the Mesæterhø Group. It is a grey-white to yellow calcite marble that shows intensive folding with hinge thickening and shearing-out along fold limbs.

STRATIGRAPHIC POSITION OF THE FOLLA AND MESÆTERHØ GROUPS

The pyritite in Grimsdalen is a stratiform horizon in a series of greenschists which represent metavolcanics intercalated with thin layers of sedimentary origin. The pyritite is therefore interpreted as being of submarine exhalative origin. This interpretation has already been applied to the belt of sulphide deposits associated with greenstones that characterizes the Scandinavian Caledonides (Oftedahl 1958, Geis 1960, Page 1964, Anger 1966, Vokes 1968, 1976, Rui 1973, Juve 1974).

The sequence basic greenschist – pyrite – quartz-keratophyre – sericitic greenschist can be regarded as representing a magmatic evolution starting with an initial series of basic eruptives followed by a period during which fractionation of a hydrothermal and an acid phase took place. The hydrothermal phase migrated away along cracks and fissures, and the heavy metals were precipitated on the sea floor (exhalative phase). The magmatogenic origin of the pyritite is supported geochemically by the occurrence of the element Te which is not found in measurable concentrations in sedimentary rocks (Sindeeva 1964). After the exhalative phase the volcanism continued with an acid extrusive phase with eruption of quartz–keratophyre. The volcanic activity ended with the deposition of a series of spilitic volcanics represented by the sericitic greenschists. According to this interpretation the Folla Group is inverted.

The composition of the clasts in the greenstone conglomerate indicates that the conglomerate was formed by erosion of the Folla Group and older rocks. It is therefore assumed that the true stratigraphical position of the Mesæterhø Group is above the Folla Group.

On the basis of the presence of the greenstone conglomerate and the marble, the Mesæterhø Group may be correlated with the Sel Mica Schist (Strand 1951) in the Sel–Vågå area. The Folla Group can then be correlated with the greenstone series of the Sel–Vågå area.

Wolff (1967) and Heim (1971) correlate the Folla Group with the Støren Group (Vogt 1945) of the Trondheim Nappe and consider the Mesæterhø Group as representing the Gula Group of the central Trondheim Region. Heim (1971) argues that the Folla Group and the Gula Group in the southern part of the south-eastern Trondheim Region are part of the same inverted nappe unit. However, as the Folla Group and the Mesæterhø Group are separated by a major thrust the present author suggests that the Folla Group is inverted, while the overlying Mesæterhø Group is lying in its original stratigraphical position in the Grimsdalen area.

The pyritite and its ore minerals

The pyrite is rather massive and ore minerals (pyrite, pyrrhotite, magnetite, sphalerite, chalcopyrite and galena) constitute more than 70% by volume. The gangue minerals are mainly quartz and calcite while chlorite, plagioclase and hornblende are usually present but only as minor constituents.

In the few fields exposures, the pyritite forms rusty bands often covered by jarosite. In fresh drill cores and hand specimens the rock is brass-yellow due to the presence of the fine-grained pyrite. Pyrrhotite in the matrix gives the rock a buff grey hue, and sphalerite is visible as red-brown stains. Magnetite forms thin black bands or schlieren in a pyritite with green-yellow colour, due to chalcopyrite in the matrix.

On the basis of the mineral parageneses (Table 1) four ore types may be distinguished:

1) pyrrhotite–pyrite ore
2) magnetite–pyrrhotite–pyrite ore
3) magnetite–pyrite ore
4) sphalerite–pyrite ore.

Pyrite is the dominant ore mineral in all ore types and constitutes 50–70 vol% of the rock. Chalcopyrite is always present in amounts of generally about 2–3%. Pyrrhotite, magnetite and sphalerite in varying amounts form characteristic constituents of the different ore types.

TYPES OF ORE

The *pyrrhotite–pyrite ore* is characterised by its large amount of pyrrhotite —

Table 1. The composition (vol.%) of the ore types as determined by microscopic point-counting analysis of polished sections with a 25 points grid integration occular. The reliability of the point-counting analysis is calculated from the method given by Kalsbeek (1969). In most samples 1000 points were counted. Sample 3078 represents cataclastically deformed ore type 4. The samples, with the numbers given, are stored at the Institut for Almen Geologi, University of Copenhagen. In addition to the minerals listed in this table all the samples contain silicates and carbonates

Ore type	Sample number	Pyrite	Pyrrhotite	Chalcopyrite	Sphalerite	Galena	Nativ Gold	Molybdenite	Cubanite	Altaite	Hessite	Marcasite	Magnetite
pyrrhotite –pyrite ore ore type 1	2795	68 ± 2	22 ± 1	2.5 ± 0.4	0.4 ± 0.2	+	+	+					1.3
	2792	54 ± 5	35 ± 3	2.4 ± 0.5	0.9 ± 0.6		+	+		+			
	2790	52 ± 5	36 ± 3	2.7 ± 0.6	0.2 ± 0.1		+	+					+
magnetite –pyrrhotite –pyrite ore ore type 2	2612	60 ± 4	13 ± 2	2 ± 0.8	2 ± 0.8			+					8 ± 2
	2794	57 ± 4	22 ± 3	2 ± 0.8	0.5 ± 0.4	+	+	+					16 ± 2
	3979	57 ± 3	3 ± 1	2.5 ± 0.8	0.7 ± 0.6			+				0.2	7 ± 2
magnetite –pyrite ore ore type 3	3085	60 ± 4		3 ± 1	0.5 ± 0.3			+					18 ± 3
	3086	49 ± 4	0.4 ± 0.2	4 ± 1	0.8 ± 0.3	+		+			+		29 ± 3
	3094	58 ± 5	0.3 ± 0.2	3 ± 1	0.3 ± 0.2			+		+			12 ± 2
sphalerite –pyrite ore ore type 4	3081	73 ± 3		0.5 ± 0.2	12 ± 0.2	0.5 ± 0.2		+	+	+	+	0.2	
	3768	63 ± 4		0.4 ± 0.2	14 ± 2	3 ± 1		+	+	+	+		
	3769	63 ± 4	0.1 ± 0.1	3 ± 1	5 ± 1	0.3 ± 0.2		+	+	+	+		0.2 ± 0.1
	2717	63 ± 3	+	1 ± 0.2	9 ± 1	2 ± 0.5		+	+	0.05 ± 0.02	0.05 ± 0.02		
	3078	54 ± 3	+		21 ± 3	+		+	+		+	2.2 ± 0.8	

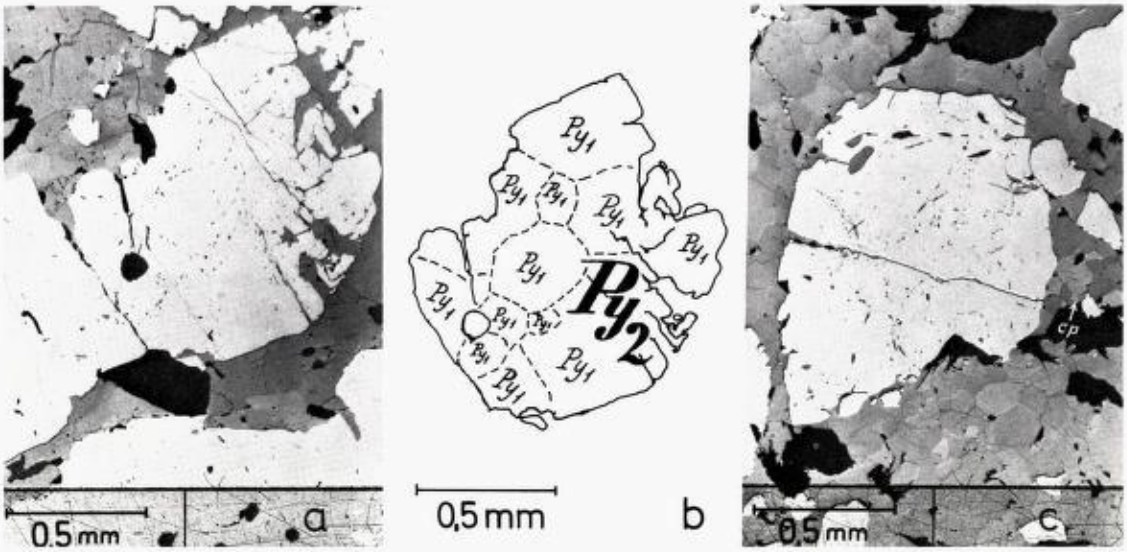

Fig. 3. Pyrrhotite–pyrite ore, ore type 1. White = pyrite, grey = pyrrhotite, black = silicates, Cp = chalcopyrite.
a) Large pyrite (py_2) grain containing traces of boundaries of py_1 grains.
b) Outline of the py_1 grains in the py_2 porphyroblast of Fig. 3a.
c) Py_2 porphyroblast in granoblastic pyrrhotite (po_2) matrix.
Optical conditions: reflected, plane polarised light, partly crossed Nicols and Nomarski interference-contrast.

some 30 vol%. A granoblastic pyrrhotite matrix contains pyrite porphyroblasts with an average size of 1–2 mm (Fig. 3), occasionally up to 1–2 cm. The pyrites form cubes which are often partly rounded and corroded by pyrrhotite (Fig. 3). Chalcopyrite and sphalerite are intergrown with the pyrrhotite matrix.

In the *magnetite–pyrrhotite–pyrite ore* a considerable amount of the pyrrhotite is substituted by magnetite. The pyrite and pyrrhotite closely resemble the pyrite and pyrrhotite of ore type 1, and the magnetite is found as 0.1 mm idioblasts that have grown preferentially in the pyrrhotite matrix (Fig. 4). The magnetite idioblasts are concentrated in small lenses (1 × 0.1 cm) and layers up to 0.5 cm thick.

In the *magnetite–pyrite ore* pyrrhotite is almost absent and apart from pyrite, magnetite is the dominant mineral. There is an enrichment of chalcopyrite (up to about 4%) which occurs as interstitial matrix between pyrite grains (Fig. 5). Ore type 3 has, in general, a cataclastic structure. The magnetite is concentrated in 1–5 mm-wide layers and lenses that cut through aggregates of pyrite. The pyrite forms grains, 0.5 mm in size, that are flattened and elongated to give the ore type a characteristic fabric. Magnetite occurs as rounded grains c. 0.1 mm in size.

The *sphalerite–pyrite ore* contains a relatively large amount of sphalerite (some 10%), whereas pyrrhotite and magnetite are absent. Pyrite aggregates (0.5 mm across) show triple junction patterns, with sphalerite as matrix between the aggregates (Fig. 6). A number of accessory ore minerals occur in this ore

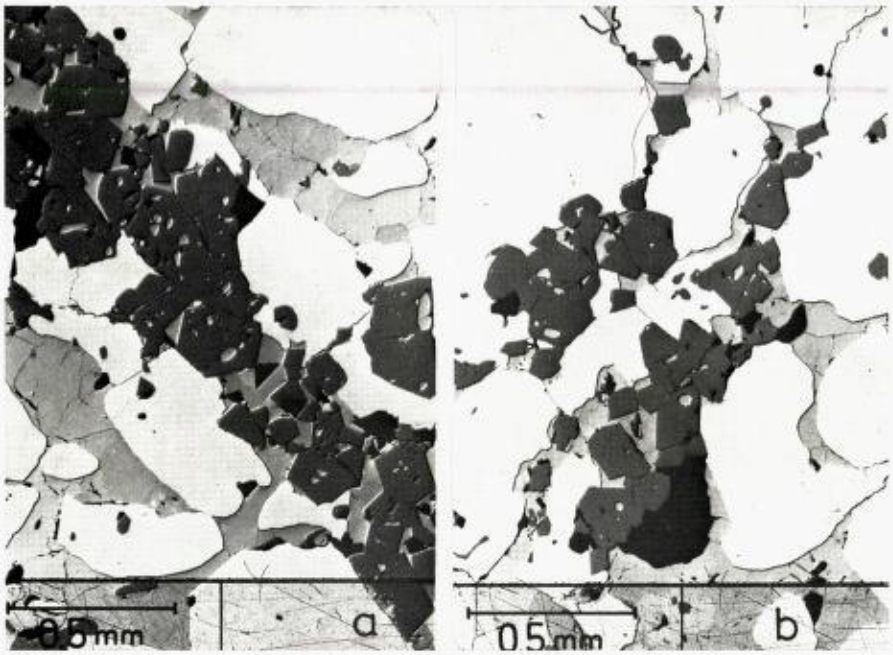

Fig. 4. Magnetite–pyrrhotite–pyrite ore, ore type 2. White = pyrite, light grey = chalcopyrite, dark grey = magnetite, black = silicates. Optical conditions: reflected, plane polarised light, partly crossed Nicols and Nomarski interference-contrast.

a) Magnetite idioblasts form a crude foliation in pyrrhotite–pyrite ore. Magnetite grew at at the expense of pyrrhotite, which occurs as inclusions in the magnetite idioblasts.

b) Magnetite idioblasts (mainly octahedra) form a diffuse foliation, from upper right to lower left, and occur predominantly in the pyrrhotite matrix.

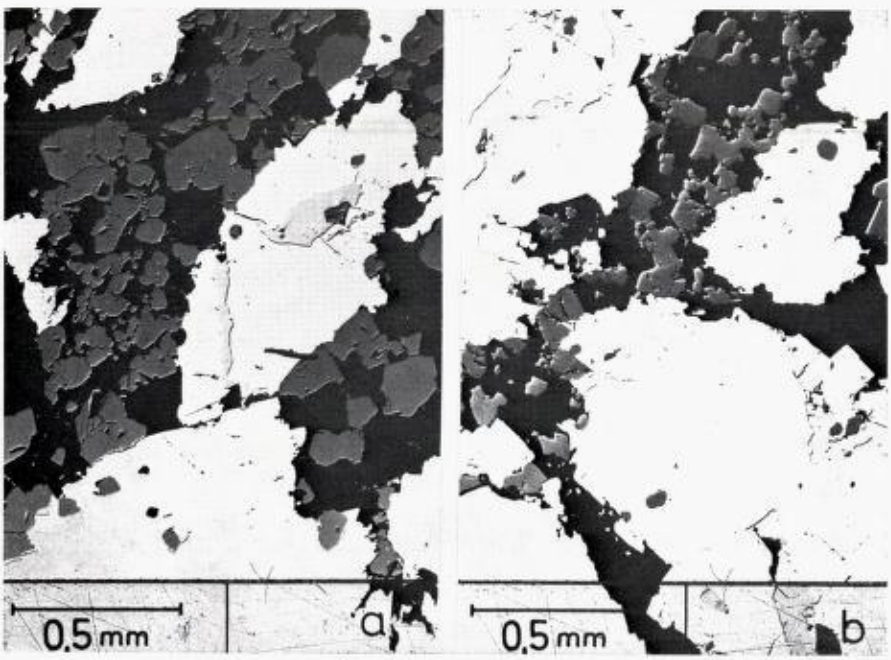

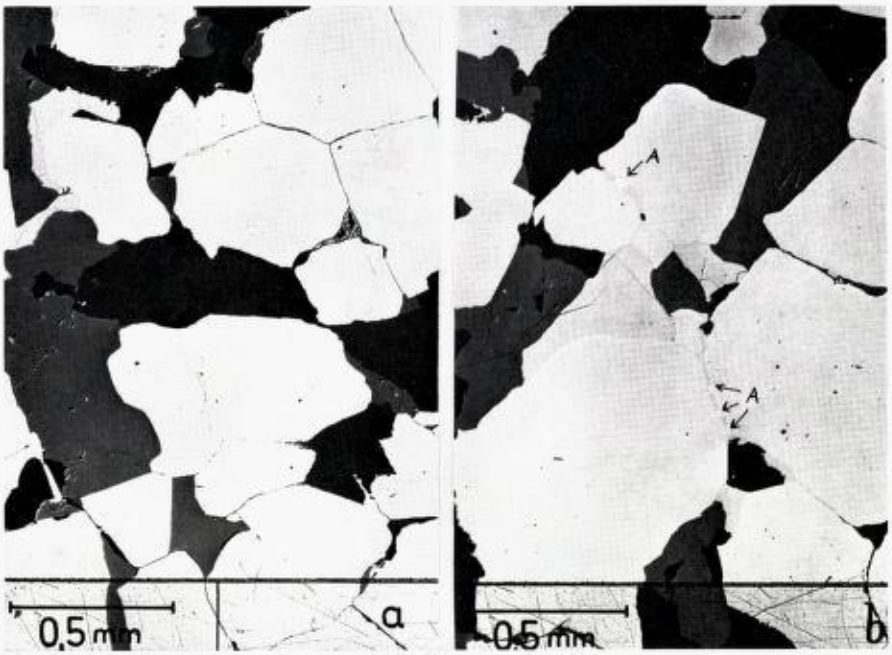

Fig. 6. Sphalerite–pyrite ore, ore type 4. White = pyrite, light grey = galena, dark grey = sphalerite, black = silicates and carbonates.
a) Typical triple junction pattern of py_3.
b) The location of altaite (A, arrowed) in galena-filled cracks between pyrite grains. Sphaerite shows weakly convex intergrown pattern with galena.
Optical conditions: reflected, plane polarised light, partly crossed Nicols and Nomarski interference-contrast.

type. Galena is the most important, besides tellurium minerals, molybdenite and cubanite. The ore type is characterized by alternation between 1–3 cm-wide bands rich in sphalerite (15–20%) and galena (2–3%) and less sphaleritic pyritite (sphalerite 5–10%, galena 1%, with chalcopyrite and pyrrhotite present, e.g. sample 3769, Table 1). Ore type 4 appears in parasitic folds on the limbs of larger isoclinal early folds (F_{D2}). Locally the sphalerite–pyrite ore is cataclastic and contains marcasite (sample 3079, Table 1; also see Fig. 8a).

ORE MINERALS

Pyrite occurs as aggregates intergrown with other sulphides or as individual grains among calcite and silicates. In aggregates with pyrrhotite and chalcopyrite, pyrite often forms cubes, but due to tectonic deformation these may be fractured and the cracks filled with chalcopyrite.

Fig. 5. Magnetite–pyrite, ore type 3. White = pyrite, light grey = chalcopyrite, dark grey = magnetite, black = silicates and carbonates. Optical conditions: reflected, plane polarised light, partly crossed nicols and Nomarski interference-contrast.
a) Elongation and flattening of pyrite due to cataclastic deformation. Magnetite grains are rounded and inclusion-free. The foliation in the rock is oriented diagonally in the picture.
b) Cataclastically deformed pyrite with interstitial chalcopyrite.

Fig. 7. Cataclastic sphalerite–pyrite ore.
White = pyrite, light grey = galena, dark grey = sphalerite, black = carbonates and silicates. Pyrite is cataclastically deformed and sphalerite has migrated into cracks and fissures.
Optical conditions: reflected, plane polarised light, partly crossed Nicols and Nomarski interference-contrast.

Four generations of pyrite formation have been recognized, termed py_1, py_2, py_3 and py_4. The outlines of py_1 are preserved by inclusions in py_2 grains. Py_2 occurs as porphyroblasts in ore types 1 and 2 (Figs. 3 and 9), and has partly been corroded by the pyrrhotite. Py_3 is found in ore type 4 as 0.5 mm grains showing 120° triple junction patterns (Smith 1964, Stanton 1972; Fig. 6), which together with the absence of inclusions indicates recrystallization under stable conditions. Py_4 occurs interstitially betwen cataclastic py_2 and py_3 grains (Fig. 8), and *marcasite* forms a concentric pattern in the central parts of py_4.

Droplets of native *gold* 0.005 mm in size and 0.01 mm-long *molybdenite* laths are found as exotic inclusions in py_2. Molybdenite is present as scattered grains up to 0.1 mm long in the ore types 3 and 4.

Small inclusions of *pyrrhotite* following the py_1 grain boundaries within the py_2 grains constitute the oldest pyrrhotite, termed po_1. Po_2 forms the matrix between py_2 grains and shows granoblastic textures (Fig. 3). Single po_2 porphyroblasts show undulating extinction and the po_2 textures resemble blastomylonites (Hobbs et al. 1976) with py_2 cataclasts.

In the magnetite-pyrrhotite-pyrite ore, pyrrhotite occurs as inclusions in magnetite idioblasts. The inclusions form drops or laths which are often orientated in the (111) directions in the magnetite.

In ore type 3 *magnetite* is concentrated in bands and lenses together with the gangue minerals quartz and plagioclase (Fig. 5). The magnetite grains have

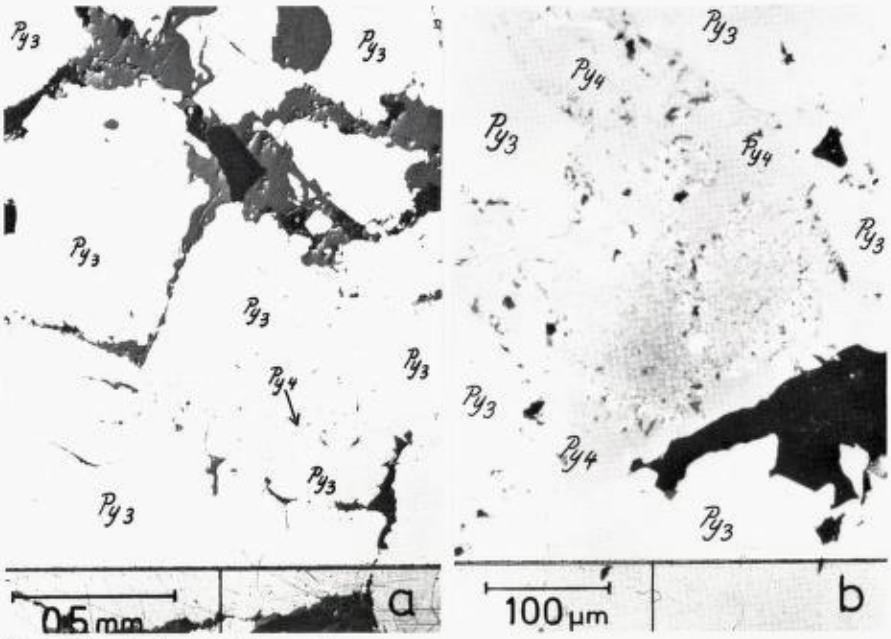

Fig. 8. Cataclastic sphalerite–pyrite ore.

a) Interstitial pyrite 4 (py_4) between pyrite 3 (py_3) grains. Dark grey = sphalerite, black = silicates and carbonates.
Optical conditions: reflected, plane polarised light, partly crossed Nicols and Nomarski interference-contrast.

b) Concentric pattern of marcasite in pyrite 4. Py_3 = pyrite 3, Py_4 = pyrite 4, dark and white angular minerals = marcasite, black = silicates and carbonates.
Optical conditions: reflected, plane polarised light, crossed Nicols and oil immersion.

a diameter of 0.01–0.1 mm and may be more or less rounded due to cataclastic deformation. In this ore type the magnetite is always clean and free of inclusions in contrast to the pyrrhotite-inclusion-rich idioblastic magnetite of ore type 2.

The content of *sphalerite* varies very much in the pyritite. In ore types 1 and 2 sphalerite occurs as an accessory mineral in the pyrrhotite matrix, and in ore type 3 it is associated with the chalcopyrite matrix. Sphalerite has been found as inclusions in py_2 where it forms inclusions together with pyrrhotite (po_1).

Apart from pyrite, sphalerite is the main mineral in the sphalerite-pyrite ore. Sphalerite behaves as a typical interstitial matrix mineral, filling spaces between py_3 grains and calcite. In the cataclastic sphalerite-pyrite ore sphalerite shows signs of great mobility, having migrated into cracks and fissures in the deformed py_3 grains (Fig. 7).

Galena is always present together with sphalerite in ore type 4, but is rarely observed in the other ore types. Sphalerite is frequently seen convexly grown into galena, a relationship which according to Stanton (1972) and Juve (1974) is due to a 'stronger' recrystallization strength of sphalerite.

The *chalcopyrite* content is greatest in the magnetite-pyrite ore; here, chalcopyrite generally occurs as the only mineral besides pyrite and magnetite. This indicates a positive correlation between chalcopyrite and magnetite (which means that when the pyritite is magnetite-banded one will always find a chalcopyrite-rich sulphide ore). In ore types 1 and 2 chalcopyrite occurs as a matrix mineral intergrown with pyrrhotite.

In the sphalerite-pyrite ore, chalcopyrite appears together with galena in the matrix. Characteristic inclusions in py_3 contain chalcopyrite + cubanite ± pyrrhotite. These inclusions reflect an exsolved intermediate solid solution (Kullerud 1969). Mackinawite/valleriite and enargite have been observed in chalcopyrite inclusions in pyrite (mainly py_3).

Tellurides occur as inclusions within, or along the boundaries of the galena grains in ore type 4. *Hessite* (Ag_2Te) and *altaite* (PbTe) form 0.01 mm grains in corners and fissures between galena and adjacent sulphides (sphalerite, pyrite and chalcopyrite). Hessite is found as 0.01 mm droplets within galena.

Tellurobismuth (Bi_2Te_3) forms small wedge-shaped lammellae in altaite or lath-shaped individual grains. The identification of altaite, hessite and tellurobismuth was based on reflectivity measurements and supported by semiquantitative microprobe scanning element determinations.

Ilmenite is common (up to 5%) in the basic greenschist, but is only present in the pyritite where the greenschist has been infolded in the pyritite. The ilmenite grains are 0.1–0.3 mm in size and often lath-shaped. In a few cases *rutile* inclusions have been found in the ilmenite. In addition, rutile occurs as single grains together with magnetite in ore type 3.

Metamorphic evolution of the pyritite

Primary structures, such as gel- or framboidal structures, that indicate formation in seawater at ordinary temperatures have not been observed in the investigated samples. It is suggested that the oldest sulphide grains $py_1 + po_1$ (Fig. 9, stage I) were generated during diagenesis or early metamorphism. The reaction $py_1 + po_1 \rightarrow py_2$ (Fig. 9, stage II) requires increasing S_2 pressure (Holland 1965, Barton 1970). Less metamorphosed stratiform exhalative sulphide deposits (Meggen, Rammelsberg and Kuroko) often contain gypsum, anhydrite or baryte (Anger et al 1966, Tatsumi 1970, Sato 1972). Therefore, it is supposed that the required increase in S_2 fugacity resulted from the breakdown of syn-depositional $CaSO_4$ which becomes unstable at higher temperatures under contemporaneous formation of other Ca-minerals, e.g. $CaCO_3$. Calcite is always present in the pyritite.

The evolution from stage II to stage III (Fig. 9) may be explained by an increase in temperature (Barton 1970), and the first three stages thus represent increasing metamorphism up to amphibolite facies conditions.

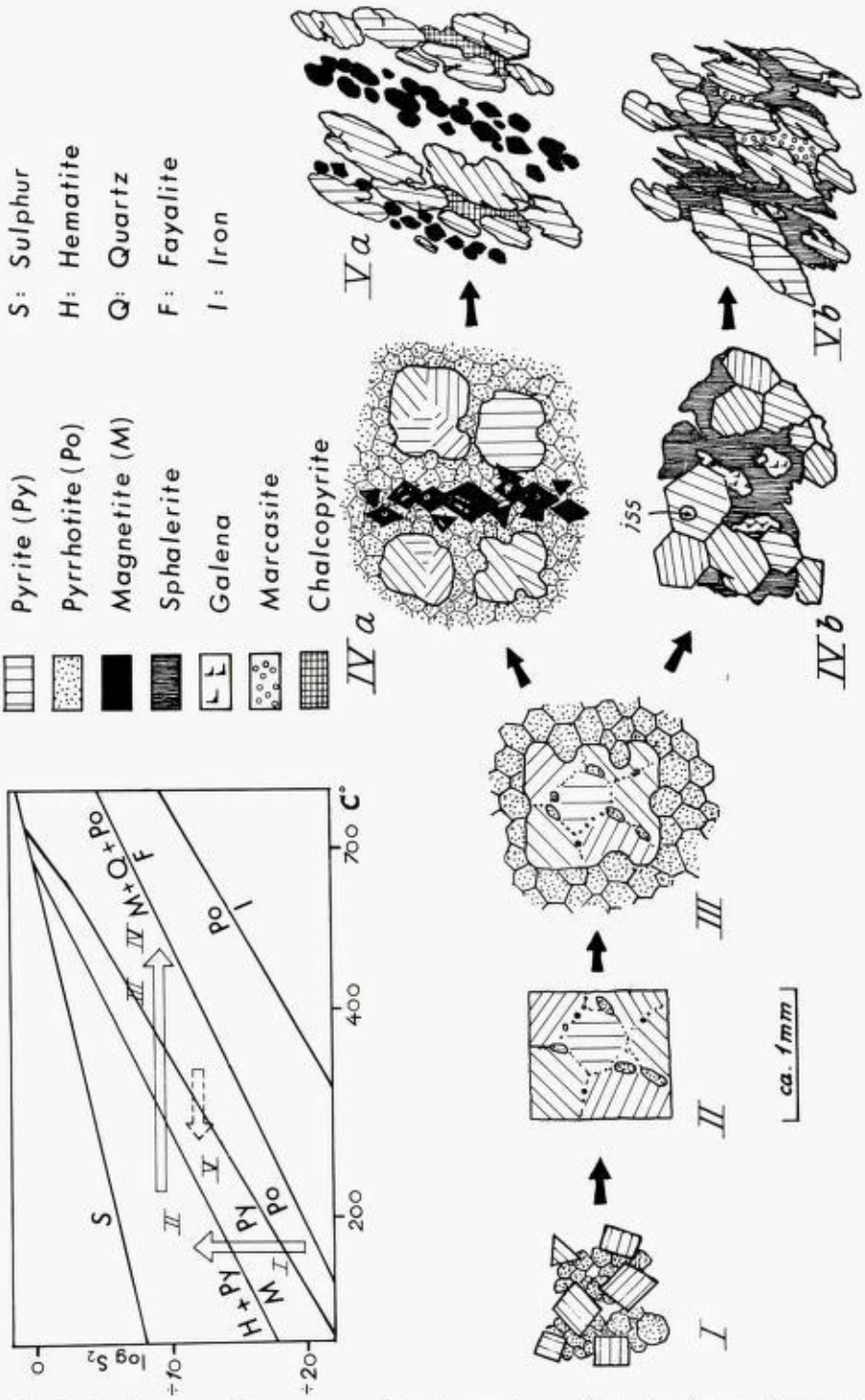

Fig. 9. Development of the ore types. The diagram is modified after Barton (1970) and shows the development of the ore types in stages in relation to temperature and sulphur fugacity (log S_2). Stage III = ore type 1, stage IVa = ore type 2, stage IVb = ore type 4, stage Va = ore type 3 and stage Vb = cataclastic ore type 4. In stage IV 'iss' refers to intermediate solid solution inclusion (chalcopyrite + cubanite ± pyrrhotite).

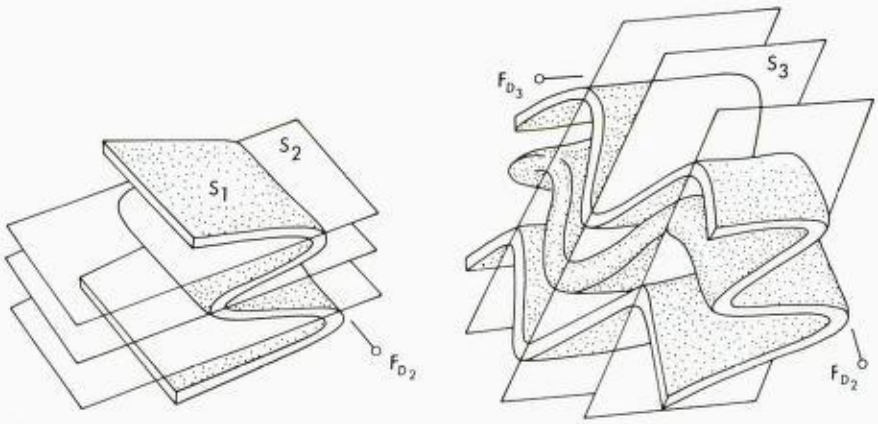

Fig. 10. Diagram to show the relationship between the structural surfaces developed during the two main deformations.

The magnetite blastesis (stage IVa, Fig. 9), and the formation of ore types 2 and 3 (stage IVa and Va), is interpreted as the result of an increase in O_2 fugacity. As pyrite was not altered during the magnetite blastesis, the S_2 fugasity must have been stable (Holland 1965, Figs. 26, 27), but the O_2 fugacity was increasing. O_2 was introduced along cleavage planes in the pyritite formed during the early fold phase, and in agreement with this magnetite layers and lenses define a foliation in the pyrite (Fig. 9, stage IVa, Fig. 4).

The sphalerite–pyrite ore (ore type 4) is concentrated in parasitic folds. The ore was recrystallized under stable conditions as shown by the triple junction pattern of py_3 (Smith 1964, Stanton 1972). Py_3 contains inclusions of chalcopyrite + cubanite ± pyrrhotite corresponding to intermediate solid solution inclusions. The estimated composition of the intermediate solid solution shows that the inclusions formed at temperatures above 400 °C (Craig & Scott 1974). This supports the idea that the concentration of the sphalerite–pyrite ore took place under amphibolite facies conditions.

A cataclastic deformation affected the pyritite whereby ore type 2 was transformed into ore type 3 (stage IVa to Va, Fig. 9). The disappearance of pyrrhotite is ascribed to decreasing temperature (Barton 1970) and the introduction of O_2 along developing cleavage planes. Chalcopyrite is separated from the disappearing po_2 matrix and remains as the only matrix mineral between the pyrite grains.

In ore type 4 cataclastic deformation (stage Vb, Fig. 9) resulted in elongation and jointing of py_3 grains, and the cracks in py_3 were filled with sphalerite. Py_4 was formed as a metastable phase which under retrograde metamorphic conditions altered to marcasite. (A supergene origin for the py_4 and marcasite can hardly be supported as the investigated samples with py_4 and marcasite were all taken from a fresh drill core below 30 m depth).

Structural and metamorphic development

The general strike in Grimsdalen is ENE and dips between 50°–70° to NNW prevail. Three main deformations have affected the area. The first deformation,

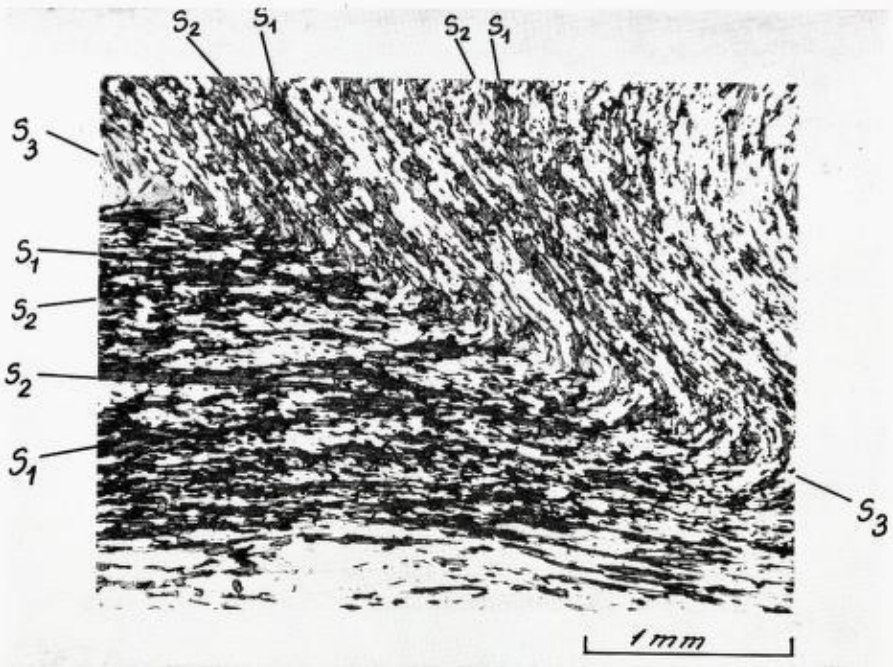

Fig. 11. Basic greenschist. The relationship between the schistosities S_1 and S_2 and the incipient cleavage S_3. S_1 and S_2 are defined by hornblende. S_3 is a poorly developed crenulation cleavage corresponding to the axial plane of the F_{D3} deformation. Neocrystallization of chlorite is just perceptible along S_3. Thin-section, plane polarised light.

D_1, is represented by the earliest recognizable schistosity, s_1. During the D_2 deformation s_1 was folded, and the axial plane schistosity s_2 developed. Finally the s_1 and s_2 schistosities were folded together by the structures belonging to the D_3 deformation, whereby the s_3 axial plane cleavage was formed (Fig. 10); this deformation is responsible for the steep dip of the rock layering to the north–northwest.

THE EARLY FOLD PHASE, F_{D2}

The earliest recognizable *folds* are isoclinal, recumbent folds with axes trending between N and NW with an overlap of up to several kilometres. The axes were more or less horizontal prior to the later folding. During the D_3 deformation the early axes were folded so that they now plunge in accordance with their position on the limbs of F_{D3} folds, generally to between N and NW (Fig. 10). A large nappe fold closure has been shown to be situated in Kakelldalen c. 10 km northeast of Folldal.

F_{D2} mesostructures can be seen in most larger exposures. Interference patterns such as arrow-head and lunar structures occur where the F_{D2} folds appear in favourable F_{D3} crests. This is especially the case where meta–quartz–keratophyre is infolded in the basic greenschist. In the sericitic greenschist F_{D2} crenulation folds have often been preserved on the limbs of F_{D3} crenulation folds, but have been wiped out on the crests.

F_{D2} microfolds are often seen in thin-section. In the mica schist the folds are defined by the bending of a biotite s_1 schistosity and in the basic greenschist of a hornblende s_1 schistosity (Fig. 11). The development of the s_2 schistosity in the garnet–biotite schist is accompanied by the formation of staurolite, kyanite and garnet. In the basic greenschist almandine occurs as idioblasts while hornblende defines the s_2 schistosity which is characterized by fewer but larger hornblende laths than s_1 (Fig. 11). As a result of the F_{D3} folding the s_1 and s_2 schistosities have been pressed together so as to be nearly parallel. Hornblende prisms also outline a lineation parallel to the F_{D2} axis. Andesine (An_{30}) has been found in a single amphibolite unit and as megacrysts in an F_{D2} fold closure. According to Turner & Verhoogen (1960) and Winkler (1967) these minerals indicate almandine–amphibolite facies metamorphism, and hence it is concluded that the early F_{D2} folding took place under similar metamorphic conditions.

THE LATE FOLD PHASE, F_{D3}

The late fold phase produced the dominant structures in the Grimsdalen area. The folds are tight to close folds which are overturned to the south with axial planes dipping c. 60°N. The general plunge of the fold axes is 10°–20° towards WSW.

The most prominent F_{D3} macrostructure is a synform with a core of basic greenschist which can be followed from Grimsdals Gruva to Mesæter where it has been displaced by a fault with both vertical and dextral displacement (Plate 1). Along the south-west side of the fault the axis of the synform shows a drag effect which indicates the direction of movement on the fault plane (subarea 10, Plate 1). South-west of the fault the synform continues to the area north of Tverrlisæter and on to the south-west below Grimsdalshytta to another fault. On the other side of this fault the structure can be followed to Verkensæter. The faulting is regarded as the latest deformation phase in the area, D_4.

The style of the fold structures seen in exposures depends very much on the lithology. The mica schist and the basic greenschist form angular folds, while the meta–quartz–keratophyre is typically buckle-folded. The sericitic greenschist is often kink-folded.

The F_{D3} microfolds are very obvious. The bending of s_1 and s_2 is locally accompanied by the development of an axial plane cleavage s_3 (Figs. 10, 11). In the greenschist chlorite forms the s_3 schistosity and it is inferred that greenschist facies conditions prevailed during the D_3 deformation. Due to this greenschist facies metamorphism sericite forms pseudomorphs after staurolite and kyanite, while garnet, hornblende and biotite are often altered to chlorite; albite is the generally occurring plagioclase. Accordingly, the deformations can be listed as in Table 2.

A tectonic model (Fig. 12) has been established for the area around Tverrlisæter (Plate 1). Field work has shown that the model is valid throughout Grimsdalen and that with few modifications it may be applied in the Folldal–Kakelldalen area. To clarify and simplify the model all units are shown as

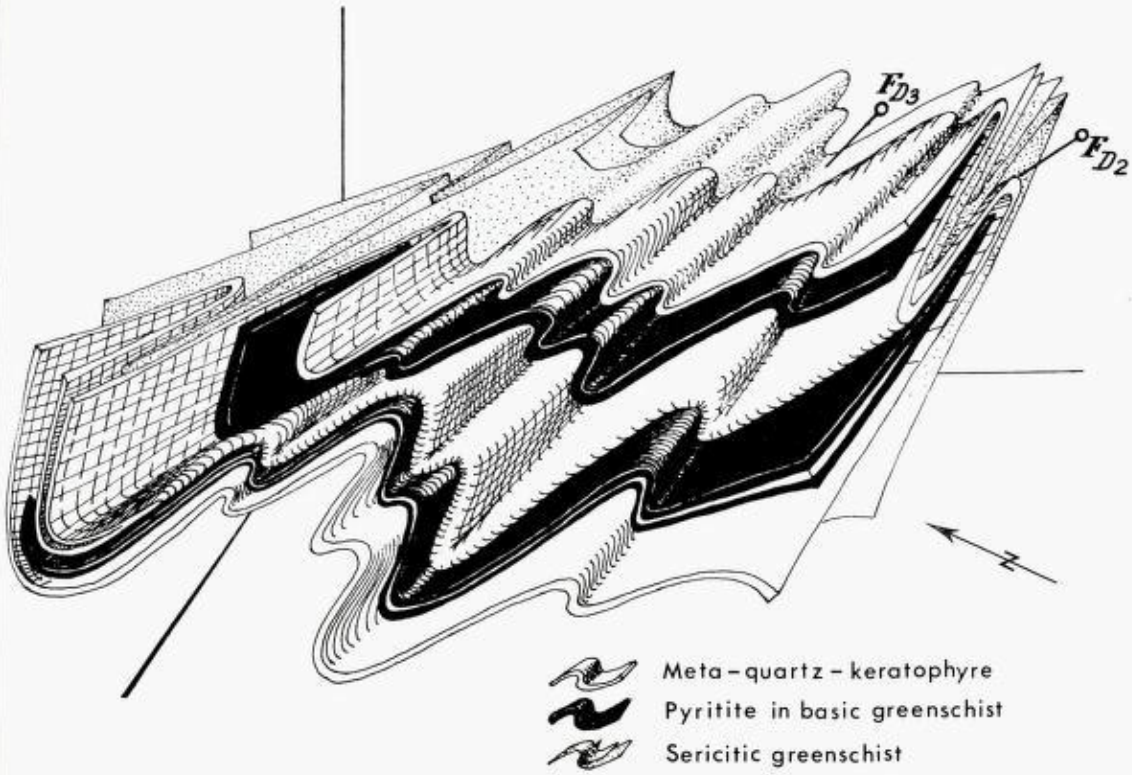

Fig. 12. Tectonic model of the fold structure at Tverrlisæter, Grimsdalen.

having constant thicknesses. In actual fact there are numerous examples of thinning of lithological units on fold limbs and increased thickness in fold hinges. These variations in thickness are most strongly developed within the pyritite.

Table 2. The structural and mineralogical characteristics of the different phases of deformation

Deformation phase	Folding	Schistosity, lineation	Metamorphism	Other deformations
D_1	None observed	s_1: hornblende, biotite	upper greenschist facies?	
D_2	F_{D2}: recumbent, isoclinal	s_2: hornblende, muscovite	amphibolite facies	thrusting along F_{D2} fold limbs, boudinage
D_3	F_{D3}: overturned, tight to close	s_3: chlorite, crenulation cleavage	greenschist facies	overthrusting to the SE
D_4	drag folding of F_{D3} axes along faults			faulting

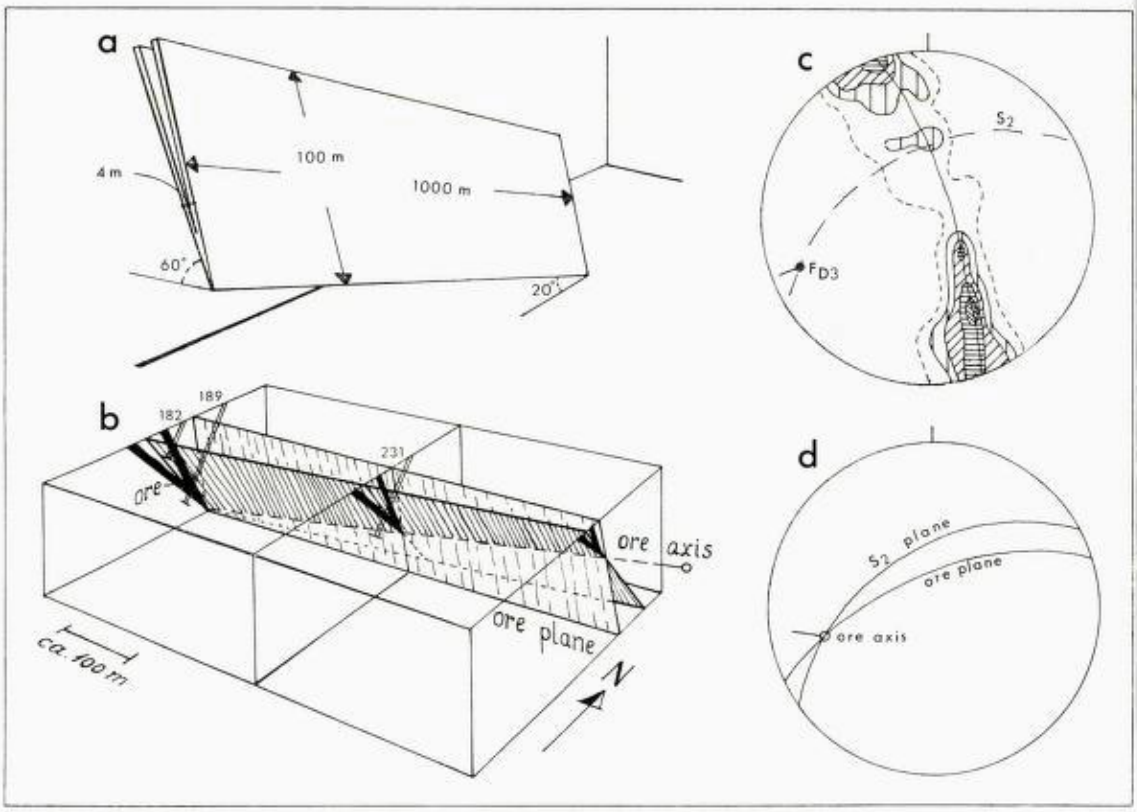

Fig. 13. Construction of the position of an ore body in the area around Tverrlisæter.
a) Idealized shape and orientation of the ore body.
b) Spatial relationship between the ore plane (dashed lines) and the general schistosity (lined). The construction of the ore axis is shown. The numbers refer to diamond drill cores (see Fig. 2).
c) The poles to the schistosity planes from the Tverrlisæter area are plotted stereographically and a general structural plane is constructed. Lower hemisphere, Wulff net. The normal to the great circle through the schistosity poles is the latest fold axis F_{D3}.
d) The intersection between the ore plane, taken from stereogram 8, Plate 1, and the S_2 plane from Fig. 13c gives the ore axis, i.e. the edge of the wedge-shaped ore body (Figs. 13a and 13b).

Tectonic control of the ore

Investigations at the Grimsdalen mine show that the ore is concentrated in the closures of isoclinal F_{D2} folds (Figs. 2 and 12). The fold cores are dominated by ore type 1 while ore type 4 is concentrated in parasitic folds on the limbs of the big F_{D2} folds. Where the pyritite has been strongly affected by the D_3 deformation the cataclastic ore types of stage V (Fig. 9) are developed.

Field evidence thus etablishes that the pyritite is concentrated in F_{D2} fold hinges. Location of ore bodies is then dependent on the distribution of F_{D2} folds within the F_{D3} pattern. The F_{D2} axes which are bent around the F_{D3} axes lie approximately on a great circle on a stereographic net as shown by diagram 8 in Plate 1. This great circle defines a plane that, for ores concentrated in early folds in refolded areas, is designated the ore plane (Stauffer 1968) (Fig. 13).

The ideal shape of an ore body will be a narrow wedge with the edge parallel to the F_{D2} axis (Fig. 13). The direction of the edge is given by the intersection of the ore plane and the dominating planar structure of the area.

Geophysical investigations carried out by Folldal Verk A/S show a complex pattern, but the anomalies caused by the pyritite can be related to the F_{D2} fold axes and to the tectonic model (Fig. 12). On the basis of the geophysical investigations diamond drilling was carried out which intersected an ore body west of Tverrlisæter. The continuation of this ore body was predicted from the tectonic model (Fig. 12), and a diamond drill core later proved the existence of the pyritite at the estimated depth.

Conclusions

The sulphide deposit in Grimsdalen is a stratiform mineralization belonging to a single pyritite horizon and related to the big group of Cu and Zn sulphide deposits of the Scandinavian Caledonides (Vokes 1976). The ore is regarded as being of exhalative–sedimentary origin and occurs in a series of metavolcanics, the Folla Group of Heim (1971), which may be correlated with the early Ordovician Støren Group. The ore-forming pyritite horizon is found in the following structural succession: (top) grenschist, pyritite, meta–quartz–keratophyre sericitic greenschist and graphite–mica schist (bottom). This sequence of the Folla Group is considered to represent an inverted stratigraphical succession, while the Mesæterhø Group lies in its original stratigraphical position above the Folla Group, though now with thrust contact.

The pyritite has been subjected to two major deformation phases. The earliest recognizable fold phase (F_{D2}, Table 2) formed recumbent, isoclinal folds under amphibolite facies conditions. During this deformation the ore types 1, 2 and 4 were formed. The pyritite was concentrated in wedge-shaped bodies in the closures of isoclinal folds.

The later fold phase (F_{D3}, Table 2) characterized by greenschist facies conditions created overturned tight to close folds. During cataclastic deformation ore type 3 and a cataclastic ore type 4 (Stage V, Fig. 9) developed. The position of the ore bodies is determined by the F_{D3} folding.

A structural model for the Grimsdalen area has been presented. On the basis of this model the position of the ore bodies may be predicted.

Acknowledgements. – The field work was supported by Folldal Verk A/S and the director, O. Husum, is thanked for his permission to publish the results. Dr. J. G. Heim and Mr. I. Killi, Folldal Verk A/S, are thanked for help and cooperation during three summers field work. The author is also indebted to Prof. dr. H. Urban (Frankfurt) and Prof. dr. A. Berthelsen (Copenhagen) for helpful discussions and good advice during the progress of the work. An earlier draft of this paper was read by Mr. G. Juve and Mr. F. C. Wolff (Norges geologiske Undersøkelse), who offered many helpful suggestions. Dr. M. Ghisler is thanked for editional assistance and Dr. T. C. R. Pulvertaft kindly improved the English text.

REFERENCES

Anger, G. 1966: Die Genetischen Zusammenhänge zwischen deutschen und norwegischen Schwefelkies–Lagerstätten unter besondere Berücksichtigung der Ergebnisse von Schwe-

felisotopen-Untersuchungen. *Clausthaler Hefte Lagerstättenkd. Geol., 3*, 115 pp.
Anger, G., Nielsen, H., Puchett, H., Ricke, W. 1966: Sulfur isotopes in the Rammelsberg Ore Deposit. *Econ. Geol., 61*, 511–536.
Barton, P. B. 1970: Sulfide Petrology. *Mineral. Soc. Amer. Spec. Pap. 3*, 187–198.
Bjørlykke, K. 1905: Det Centrale Norges Fjeldbygning. *Norges geol. Unders. 39*, 595 pp.
Bugge, C. 1954: Den Kaledonske fjellkjede i Norge. *Norges geol. Unders. 189*, 79 pp.
Craig, J. R. & Scott, S. D. 1974: Sulfide phase equilibria, 109 pp. *In Sulfide Mineralogy. Mineralogical Society of America Short Course Notes.*
Foslie, S. 1926: Norges Svovelkisforekomster. *Norges geol. Unders. 127*, 122 pp.
Geis, H. P. 1960: Frühorogene Sulfidlagerstätten. *Geol. Rundsch. 50*, 46–52.
Heim, J. G. 1971: Zur Geologie des südlichen Trondheim-Gebietes. *Unpublished thesis, Johannes Gutenberg Universität, Mainz.* 154 pp.
Higgins, M. W. 1971: Cataclastic Rocks. *U.S. Geol. Survey Prof. Paper 687*, 97 pp.
Hobbs, B. E., Means, W. D. & Williams, P. F. 1976: An Outline of Structural Geology. *John. Wiley & Sons, Inc. New York.* 571 pp.
Holland, H. D. 1965: Some applications of thermochemical data to problems of ore deposits. *Econ. Geol. 60*, 1101–1167.
Juve, G. 1974: Ore Mineralogy and ore types of the Stekenjokk deposit, Central Scandinavian Caledonides, Sweden. *Sveriges geol. Unders., ser. C 706*, 162 pp.
Kalsbeek, F. 1969: Note on the reliability of point counter analyses. *N. Jahrb. Mineralogie. Monatshefte 1*, 1–6.
Kullerud, G., Yund, R. A. & Moh, G. H. 1969: Phase relations in the Cu-Fe-S, Cu-Ni-S and Fe-Ni-S system. *In* Wilson, H. D. B. (ed.) *Magmatic Ore Deposits. Econ. Geol. Monogra. 4*, 323–343.
Oftedahl, C. 1958: A Theory of Exhalative–Sedimentary Ores. *Geol. Fören. Förhandl. Stockholm, 80*, 1–19.
Page, N. J. 1964: The sulfide deposit of Nordre Gjetryggen Gruve, Folldal, Norway. *Norges geol. Unders. 228*, 217–269.
Rui, I. J. 1973: Geology and structures of the Røstvangen sulphide deposits in the Kvikne district, central Norwegian Caledonides. *Norsk geol. Tidsskr. 53*, 433–442.
Sato, T. 1972: Behaviours of ore-forming solutions in seawater. *Min. Geol. 22*, 31–42.
Schermerhorn, L. J. G. 1970: The Deposition of Volcanics and Pyritite in the Iberian Pyrite Belt. *Mineral. Deposita 5*, 273–279.
Sindeeva, N. D. 1964: Mineralogy and types of deposits of Selenium and Tellurium. *Interscience Publishers*, 363 pp.
Smith, C. S. 1964: Some elementary principles of polycrystalline microstructure. *Met. Rev. 9*, 1–33.
Stanton, R. L. 1972: Ore Petrology. *McGraw-Hill, New York*, 713 pp.
Stauffer, M. R. 1968: The tracing of hinge-line ore bodies in areas of repeated folding. *Canadian Journ. Earth Sci. 5*, 69–79.
Strand, T. 1951: The Sel–Vågå map areas. *Norges geol. Unders. 178*, 177 pp.
Strand, T. 1960: The pre-devonian rocks and structures in the region of Caledonian deformation. *In* Holtedahl, O. (ed.) *Geology of Norway. Norges geol. Unders. 208*, 170–284.
Strand, T. 1972: Scandinavian Caledonides of Norway. *In* Strand, T. & Kulling, O. (eds.): *Scandinavian Caledonides. Wiley Interscience*, 302 pp.
Tatsumi, T. 1970 (ed.): Volcanism and Ore Genesis. *University of Tokyo Press*, 448 pp.
Turner, F. J. & Verhoogen, J. 1960: Igneous and metamorphic petrology. *McGraw-Hill, New York*, 535 pp.
Vogt, T. 1945: Geology of part of the Holonda–Horg district, a type area in the Trondheim Region. *Norsk geol. Tidsskr. 25*, 449–527.
Vokes, F. M. 1968: Regional metamorphism of the palaeozoic geosynclinal sulphide deposits of Norway. *Trans. Inst. of Mining and Metall, 77*, B 53–B 59.
Vokes, F. M. 1976: Caledonian massive sulphide deposits in Scandinavia: a comparative review. *In* Wolf, K. H. (ed.): *Handbook of stratabound and stratiform ore deposits. II. Regional studies and specific deposits, Vol. 6*, 79–123. *Elsevier Scientific Publishing Company.*
Winkler, H. G. F. 1967: Petrogenesis of metamorphic rocks. *Springer-Verlag.* 237 pp.
Wolff, F. C. 1967: Geology of the Meråker area as a key to the eastern part of the Trondheim region. *Norges geol. Unders. 245*, 123–146.

Geological map of the Grimsdalen – Folldal area

Southern part of the Trondheim Region, Norway, with 14 contoured fold axis diagrams

Tverrfjell
railroad
Hjerkinn st.
Hjerkinn lake
To Dombås
9°40'E
62°14'N
Trondheim
Bergen
Oslo
Stavanger
Folla
Pighetta
Mesæterhö
Grimsdals Gruva
Mesæter
Tverrlisæter
Grimsdalshytta
Sjöberget
Storberget
Graphö
Katuglehö
Verkensæter
Tverrbekken
Tollevshaug
Grimsa
Gåsdal
Storhö
Kakelldalen
Husumbekken
Hovedgruva
Folldal
N. gruva
Geitryggen
S. gruva
Knutshovda
Nygruva
TF: thrust – fault plane of the Grimsdalshytta fault
F: fault plane of the Mesæter fault
S.S.P. 78
N
0 1 2 3 4 5 Km

1	61	30°→5°	1 3 5 7 8
2	113		1 3 4 5 6
3	83	314°→58°	1 3 5 7
4	57	72°→	1 5 15 20
5	195	262°→21°	1 3 5 10 15
6	116		1 3 5 7 10
7	114	255°→21°	1 3 5 10 13
8	169		1 3 5 10 14 16
9	88		1 3 6 9 12 15
10	132		1 3 5 7 8
11	68	256°→30°	1 3 5 7 10 13
12	43		2 5 7 10
13	24		4 8 12 15
14	109		1 2 4 6 8

Mesæterhö Group
- garnet – biotite schist
- metaconglomerate
- marble

Folla Group
- greenschist
- meta-quartz-keratophyre
- Sparagmite
- thrust
- strike and dip
- fault
- sulphide mine
- sæter

subarea 3 — contour interval (%) 1 3 5 7
number of measurements 83 — plunge of fold axis maximum 314°–58°

name of subarea
1 Mesæterhö Group
2 Thrust zone below Mesæterhö Group
3 N. Tverrâi
4 N. Tverrbekken
5 Storberget
6 Fault zone at Grimsdalshytta
7 Grimsdalshytta
8 Tverrlisæter
9 S. Tverrbekken
10 Mesæter
11 Grimsdals Gruva
12 Sjöberget
13 Nygruva – Knutshovda
14 Folldal – Kakelldalen

Plate 1. Geological map of the Grimsdalen – Folldal area. The stereograms show the axial orientations of F_{D3} folds (largest concentration) and a more diffuse great circle pattern due to the bending of the F_{D2} axes. The ornamentation representing the Folla Group greenschist depicts the style and vergence of the F_{D3} folds (looking down-plunge).